UNIVERSITI MALAYSIA PERLIS

International Journal of Nanoelectronics and Materials

IJNeaM

ISSN 1985-5761 | E-ISSN 2232-1535

Sodium Alginate/Graphene Nanoplatelet Nanocomposites: Effect of Crosslinker and Graphene Nanoplatelet Loading

Kean Chong Lim[a,b], Syarifah Nuraqmar Syed Mahamud[a,b,*] and Muhammad Afiq Zikry Badrolhisham[a,b]

[a]*Faculty of Chemical Engineering & Technology, Universiti Malaysia Perlis (UniMAP), Arau, Perlis 02600, Malaysia*
[b]*Biomedical and Nanotechnology Research Group, Center of Excellence Geopolymer and Green Technology (CEGeoGTech), Universiti Malaysia Perlis, 01000 Kangar, Perlis, Malaysia*
**Corresponding author. Tel.: +6010-203 8933; e-mail: nuraqmar@unimap.edu.my*

ABSTRACT

In this article, the effect of crosslinker and filler loading on the properties of sodium alginate/graphene nanoplatelet (SA/GNP) nanocomposites is investigated. The nanocomposites samples were prepared using the solvent casting method. Swelling tests were performed to measure the degree of swelling. It was found that the degree of swelling increased with a longer immersion time in the 0.2M concentration of $CaCl_2$. Interestingly, only a 12-minute immersion time in the 0.8M concentration of $CaCl_2$ resulted in the lowest degree of swelling, which was 93.69%. Analysis of the gel fraction showed an increase in gel content at higher $CaCl_2$ concentrations. To crosslink the SA/GNP nanocomposites, a concentration of 0.8 M $CaCl_2$ and an immersion time of 12 minutes were selected. When the mechanical properties of SA with different $CaCl_2$ concentrations were investigated, it was found that SA crosslinked at the 0.8M concentration had a higher elastic modulus than the 0.2M concentration of $CaCl_2$, which was probably due to the higher crosslinking density. The mechanical properties of SA/GNP nanocomposites were found to decrease with decreasing GNP loading, which can be attributed to the presence of GNP. In addition, higher GNP loading resulted in improved electrical conductivity of the SA/GNP nanocomposites. X-ray diffraction (XRD) analysis proved that the crystallinity of SA increased with longer immersion times and the addition of GNP. Fourier transform infrared spectroscopy (FTIR) showed no significant changes in the peak characteristics of SA when the concentration of $CaCl_2$, immersion time and GNP loading increased.

Keywords: *Sodium Alginate, Calcium Chloride, Graphene Nanoplatelet, Electrical Conductivity*

1. INTRODUCTION

Nowadays, many things are made of polymer in our life. Polymer is a macromolecule that is made up of many small repeating units called monomers linked together by covalent bond [1]. Polymers have a variety of properties depending on their structure that can modified for different uses. In recent decades, the usage of biopolymer materials in pharmaceutical and medical device applications has been growing. In addition, the versatility of biopolymer materials allowed for the design of specific biodegradable characteristics to control drug release, develop resorbable devices, and enhance cell integration. Biopolymers are a particular kind of polymer that is created from organic, renewable resources like plants and animals. Beyond biological uses, they have a wide range of applications. They are employed in the packaging industry to create biodegradable packaging materials including bags, wraps, and containers using biopolymers like cellulose and starch. They serve as an environmentally friendly substitute for conventional plastic packaging. Bioplastics are biodegradable plastics that may be used as an alternative to conventional plastics derived from fossil fuels. Biopolymer materials are used because they are versatile, simple to fabricate, biocompatible, and exhibit a wide range of mechanical, electrical, chemical, and thermal properties when combined with other materials to make composites [2]. To protect the electronic circuit of the implanted device from moisture and ions inside the human body, gas permeability and water permeability of the packaging polymer are the main criteria for biocompatible and biostable polymers used to package implanted devices. Additionally, biopolymer materials must be able to contain the device during the anticipated implant lifetime and have a high tensile strength [3]. In the case of substrates, structural and, occasionally, electrical conductivity properties would be of higher importance.

Alginate is a biopolymer made from brown seaweed. It is a repeating linear polysaccharide consisting of the sugars mannuronic acid and glucose. Numerous industries use alginate for a variety of purposes. Besides that, polymers are used as fillers to enhance their properties. Polymer material that is added with nanoparticles to enhance the properties is defined as nanocomposites. Graphene nanoplatelet (GNP) is an example of nanoparticle. GNP is a form of graphene, which is a single sheet of carbon atoms organised in a hexagonal lattice. By adding GNP into the polymer matrix, it will enhance the strength and electrical conductivity of the polymer [4].

In this research, the effect of crosslinker in the alginate film and the addition of GNP in the SA nanocomposites was evaluated and the studies of structural, mechanical properties, and electrical conductivity were done by several characterization techniques. The samples were prepared by using solvent casting. These biopolymer nanocomposites will give many advantages in many fields.

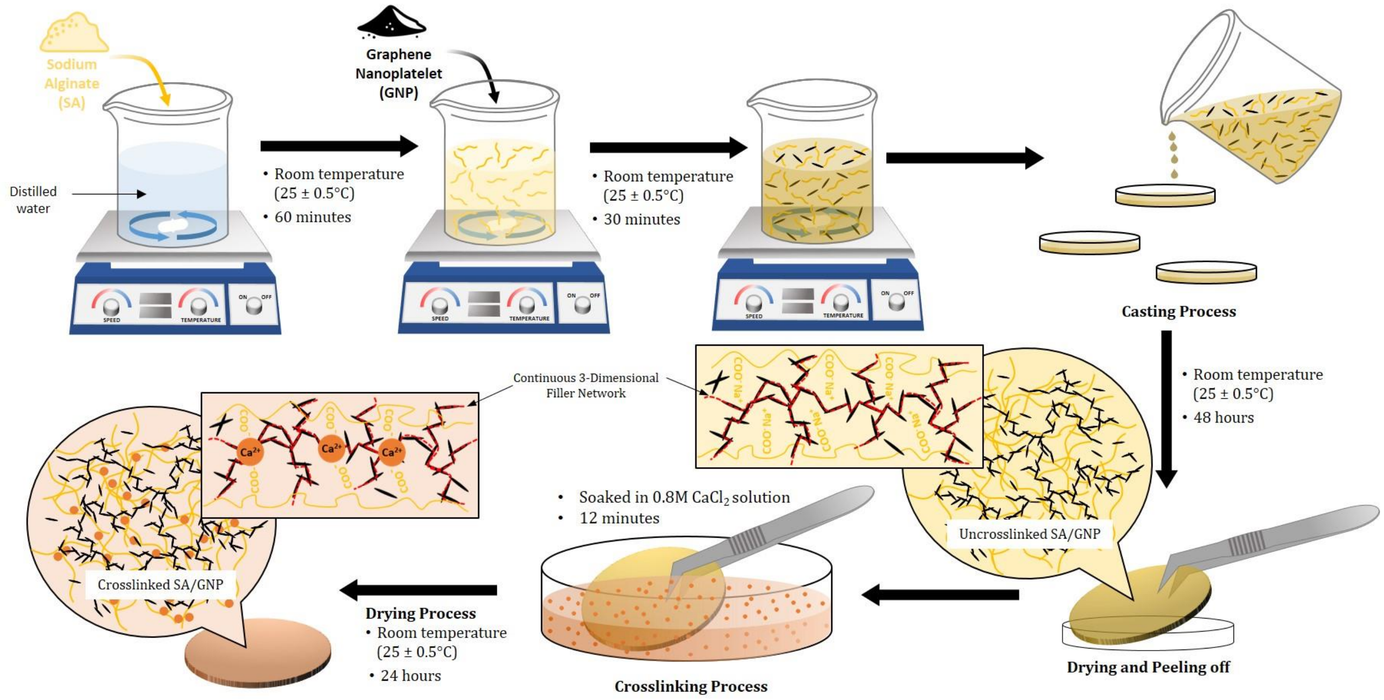

Figure 1. A schematic diagram of sodium alginate/GNP film preparation and crosslinking process.

2. EXPERIMENTAL DETAILS

2.1. Materials

Sodium alginate (SA) powder was supplied by KIMICA Corporation. Graphene nanoplatelet (GNP) with 25μm particle size was supplied by Sigma Aldrich. Calcium chloride ($CaCl_2$) was supplied by R&M chemicals.

2.2. Sample Preparation

2.2.1. Sodium Alginate (SA) Film Preparation

Sodium alginate (SA) film was prepared via solvent casting. Firstly, sodium alginate was dissolved in distilled water (0.0926 M) under constant stirring at room temperature (25 °C) for 60 min. After that, the SA solution was poured into the casting mould and left at room temperature for 48 hours to avoid sample cracking from fast drying. The uncrosslinked SA film was obtained after complete evaporation of the solvents.

The SA films were then cross-linked by immersion in a 0.2 M and 0.8 M $CaCl_2$ solution for 4, 8 and 12 minutes, respectively. The films were dried at 25 °C for 24 hours after cross-linking. The SA film with the best concentration of $CaCl_2$ solution and the best immersion time in the $CaCl_2$ solution was selected based on the physical properties for further determination of the optimal GNP loading in SA/GNP nanocomposites. Table 1 shows the concentration of $CaCl_2$ and the immersion time in $CaCl_2$.

Table 1. The concentration of $CaCl_2$ and immersion time in $CaCl_2$

Sample	$CaCl_2$ Molarity (M)	Immersion time in $CaCl_2$ (min)
Uncrosslinked SA	0	0
SA 0.2M-4min	0.2	4
SA 0.2M-8min		8
SA 0.2M-12min		12
SA 0.8M-4min	0.8	4
SA 0.8M-8min		8
SA 0.8M-12min		12

2.2.2. Sodium Alginate/Graphene Nanoplatelet (SA/GNP) Nanocomposites Film Preparation

SA/GNP nanocomposites films were prepared by solvent casting (Figure 1). First, sodium alginate was dissolved in distilled water (0.0926 M) with constant stirring at room temperature (25 °C) for 60 minutes. The SA solution was mixed with different GNP loadings (0, 4, 8, 12 wt.%) and stirred for 30 minutes. Table 2 shows the formulation of the SA/GNP nanocomposites films. The SA/GNP solution was then poured into a mould and allowed to dry at room temperature for 48 hours. The SA/GNP film was obtained after the complete evaporation of the solvents. The SA/GNP films were then crosslinked by immersion in a solution with a $CaCl_2$ concentration and immersion time based on the optimal physical performance (0.8 M $CaCl_2$ and 12 minutes immersion time). After crosslinking, the SA/GNP films were dried at 25 °C for 24 hours.

Table 2. Formulation of the SA/GNP nanocomposites film

Sample	SA (wt.%)	GNP (wt.%)
Pristine SA	100	0
SA/GNP4	96	4
SA/GNP8	92	8
SA/GNP12	88	12

2.3. Testing and Characterizations

The electrical conductivity of the samples was measured using a Fluke 8845A/8846A 6.5-digit precision multimeter with a 5 V power supply. The samples had a diameter of 15 to 20 mm and a thickness of approximately 1 mm. A layer of conductive silver paint was applied to the top and bottom of the sample to ensure good surface contact between the sample and the electrode. The electrical conductivity was measured using Equations (1) and (2).

$$Bulk\ volume\ resistivity, \Omega.\text{cm} = \left(\frac{R \times A}{t}\right) \tag{1}$$

$$Bulk\ volume\ conductivity, 1/(\Omega.\text{cm}) = 1/\left(\frac{R \times A}{t}\right) \tag{2}$$

where R is the volume resistance (Ω), A is the surface area of the sample (cm^2), and t is the sample thickness (cm).

To measure the swelling of the samples, the SA films (20 mm × 20 mm) were immersed in phosphate-buffered saline (pH 7.2). After the film had been immersed for 24 hours, the samples were carefully removed, wiped with filter paper to remove excess phosphate buffer saline from the surface, and weighed again. The percentage swelling was calculated using Equation (3).

$$\text{Swelling (\%)} = \frac{(M_W - M_0)}{M_0} \times 100 \tag{3}$$

where M_w is the final weight of samples and M_0 is the initial weight of the sample.

In this study, the gel content was measured for the cross-linked SA. The SA films were cut into 20mm × 20mm and oven dried at 60°C for 24 hours. The initial weight of the sample (W_1) was taken, and the sample was allowed to swell in 20 mL of a phosphate buffer salt solution at room temperature for 24 hours. The sample was then oven-dried at 60 °C for 24 hours until the moisture was completely removed from the samples. The final weight of the sample (W_2) was then determined. The gel content was calculated using Equation (4):

$$\text{Gel content (\%)} = \frac{W_2}{W_1} \times 100 \tag{4}$$

where W_2 is the weight of the sample after being immersed in phosphate buffer saline and W_1 is the weight of the sample after drying in the oven.

Fourier transform infrared spectroscopy (FTIR) spectra of chemical structure analysis of SA/GNP nanocomposites were obtained using Perkin-Elmer Spectrum 400 Series equipment. The scanning range and spectral resolution that were used were 4 cm^{-1} and 650-4000 cm^{-1}, respectively.

X-ray diffraction (XRD) patterns were obtained using a Bruker D2 Phaser XRD Analyzer with monochromic CuKα (λ = 1.5418) radiation. The data was collected in 2θ continuous mode at a scan rate of 0.1°/min over an angular range of 5° to 60°. The films' basal spacing (d) was calculated using the crystal orientation ratio and the Bragg's Law formula, as shown in Equations (5) and (6),

$$I = \frac{I_2}{I_1} \tag{5}$$

where I is the crystal orientation ratio of the crystal planes, I_2 is the intensity peak number 2, and I_1 is the intensity peak number 1.

$$n\lambda = 2d \sin\theta \tag{6}$$

where is the distance between atoms, λ is the wavelength of the incident radiation, and θ is the incidence angle.

The tensile test was performed following ASTM D882 using an Instron 5542 and the Bluehill v. 2.17 software package (Instron Corp., Norwood, MA, USA). Dumbbell-shaped specimens (60 × 10 × 1 mm) were prepared with a clamping distance of 40 mm the average of the three best measurements was determined. The test was performed at a crosshead speed of 5 min^{-1} at room temperature.

3. RESULTS AND DISCUSSION

3.1. Effect of $CaCl_2$ as Crosslinker on the Swelling Properties of SA

Figure 2 shows the degree of swelling of the SA films cross-linked with the different concentrations of $CaCl_2$ and immersion time. Based on Figure 2, a higher concentration of crosslinker 0.8M reduce the swelling degree of SA film. When the concentration of crosslinker is increased, there are more crosslinking points within the polymer network.

Figure 2 shows that the degree of swelling decreases as the immersion time in 0.2M $CaCl_2$ concentration is increased. the 12-minute immersion time has the lowest degree of swelling at 181.50 %, compared to the 4-minute and 12 and 8-minute immersion times at 292.73 % and 199.00 %, respectively. This is due to the structure of the SA chains, which are cross-linked by calcium, making it difficult for the phosphate buffer saline (PBS) solution to penetrate. If the PBS solution has difficulty penetrating the cross-linked SA, less PBS solution is absorbed into the free volume of the SA film

Theoretically, a higher concentration of crosslinker can lead to a faster crosslinking reaction. At 0.8M of $CaCl_2$, the 4 min immersion time of the film may not have enough time to form a tightly crosslinked structure, allowing for more solution absorption, even though the crosslinking reaction happens faster. This suggests that higher $CaCl_2$ concentration might not enable complete crosslinking in the film during a short immersion time. Elevated swelling percentages can be caused by incomplete crosslinking, which can leave more open sites for the solution to enter. The swelling degree was decreased to 121.56% when the increasing of 8 min immersion time in 0.8M concentration of $CaCl_2$. This is because when both immersion time and crosslinker concentration increase, more crosslinking sites are produced, which increases the crosslink density. The mobility of polymer chains is restricted and the amount of free volume inside the polymer network is decreased by a higher crosslink density [5]. The swelling agent encounters higher swelling resistance, as a result, leading to decreased swelling properties. Besides that, 12 min immersion time in 0.8 M concentration of $CaCl_2$ has the lowest swelling degree with 93.69%. This is because the absorption of PBS solution into the SA film will decrease as the concentration of $CaCl_2$ increases. This proves that SA with 12 min immersion time in 0.8M concentration of $CaCl_2$ is the ideal parameter to crosslink SA. 0.8M concentration of $CaCl_2$ and 12 min immersion time was selected to crosslink the SA/GNP nanocomposites.

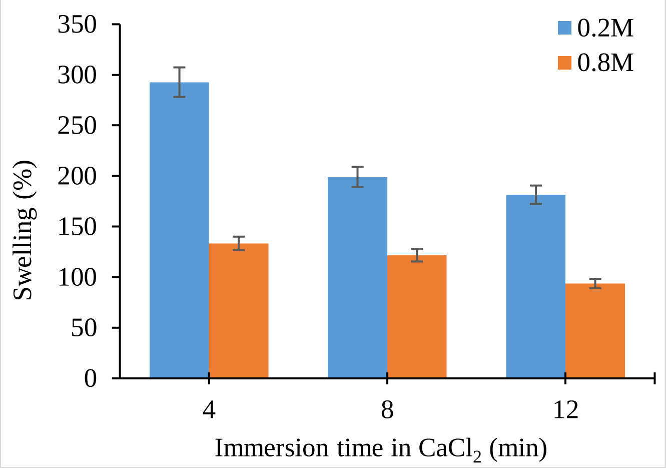

Figure 2. The swelling degree of SA with different concentrations of $CaCl_2$ and immersion time.

3.2. Effect of $CaCl_2$ as Crosslinker on the Gel Content of SA

The gel content of the SA films with different concentrations of $CaCl_2$ and immersion time is shown in Figure 3. The gel content was used to analyse the degree of cross-linking of the polymer chains in the SA films. Figure 3 shows that the 0.8M $CaCl_2$ concentration has a higher gel fraction than the 0.2M $CaCl_2$ concentration. A comparison between SA films in 0.2M and 0.8M $CaCl_2$ concentration at a fixed immersion time shows that the gel content increases with increasing $CaCl^2$ concentration. According to Ibrahim et al. the percentage of gel increases as the CaCl2 concentration increases [6]. This is due to the cross-linking of the carboxylate group of the sodium alginate with the Ca2+ ions (Figure 1).

After 4 min of immersion, the gel content of SA in 0.8M $CaCl_2$ is higher (101.80%) than that of SA in 0.2M $CaCl_2$ (92.93%). After 8 min of immersion time, SA in 0.8M $CaCl_2$ shows no significant difference in gel content compared to SA in 0.2M $CaCl_2$ (101.8% and 101.7%, respectively). When immersed for 12 minutes, SA in a 0.8M $CaCl_2$ concentration had a higher gel content (104.11%) than SA in a 0.2M $CaCl_2$ concentration (102.91%), respectively.

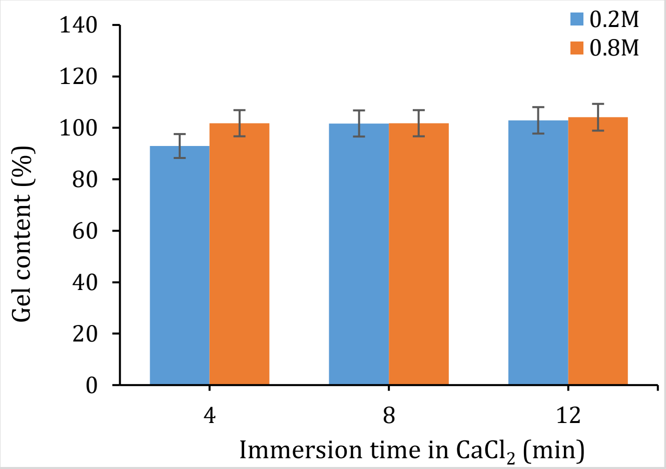

Figure 3. The gel content of SA with different concentrations of $CaCl_2$ and immersion time.

3.3. Mechanical Properties of SA with Different $CaCl_2$ Concentrations and Immersion Time

Figure 4, Figure 5 and Figure 6 demonstrate the effect of different $CaCl_2$ concentrations and immersion times on the tensile properties of SA films. According to Figure 4, the tensile strength of SA films decreases with increasing concentrations and immersion times in $CaCl_2$. Uncrosslinked SA typically has higher chain mobility and flexibility because the polymer chains are not bound together by cross-links. This increased flexibility may allow the film to undergo greater deformation before failure, which might give the appearance of higher tensile strength. The tensile strength of crosslinked SA films was progressively reduced from 23.4 MPa to 15.0 MPa with increasing immersion times in 0.2M $CaCl_2$ from 0 min to 12 min. This represents a 36% decrease in comparison to uncrosslinked SA films. In 0.8M $CaCl_2$, the crosslinked SA film showed a similar decreasing trend as immersion time increased, dropping from 23.4 MPa to 13.35 MPa, as well as 43% less than the uncrosslinked SA. High crosslinker concentrations and longer immersion times can cause the SA film to become less ductile and more rigid. The resulting material may become more brittle, reducing tensile strength because the film is less capable of accommodating deformation before failure. Obviously, at a constant immersion time, the crosslinked SA film in 0.2M $CaCl_2$ has a higher tensile strength than the crosslinked SA film in 0.8M $CaCl_2$. This is because SA 0.8M $CaCl_2$ become stiffer and brittle when more crosslinking bonds are formed between the polymer chains [6]. Crosslinking can weaken the intermolecular interactions within the polymer chains [7]. This can lead to reduced tensile strength as the chains are less able to resist applied tension forces. Uncrosslinked SA films, without these restrictions, may have stronger intermolecular interactions contributing to higher tensile strength. When the immersion time of SA in $CaCl_2$ increased, more network bonds formed due to the crosslinking process. This will decrease the tensile strength [8].

Figure 5 shows the elongation at break of uncrosslinked SA and crosslinked SA film with different $CaCl_2$ concentrations and immersion times. Uncrosslinked SA has the highest elongation at break at 17% compared with crosslinked SA. When the immersion time increases, the elongation at break for SA film immersed in either 0.2 M or 0.8 M $CaCl_2$ shows a pattern of decreasing. As the immersion time increased from 0 min to 12 min, the elongation at break for SA film in 0.2M $CaCl_2$ reduced to 8.35% while for SA in 0.8M $CaCl_2$ reduced to 7.36%. This is since increasing $CaCl_2$ concentrations and immersion times create more crosslinking sites between the polymer chains, making SA film stiffer and less able to elongate before breaking [9]. Furthermore, the crosslinking process has the potential to affect the film's hydration behaviour. Uncrosslinked films may absorb water more easily, resulting in increased flexibility and elongation.

Figure 6 shows the modulus of elasticity for uncrosslinked SA and crosslinked SA with different $CaCl_2$ concentrations and immersion times. Based on the results, both $CaCl_2$ concentrations successfully improved the elastic modulus of the SA film. By immersed SA film in 0.2M $CaCl_2$, the film shows an increase in elastic modulus. However, as the immersion time increased from 4 min to 12 min, the elastic modulus of the SA film exhibited a decreasing trend. This pattern of changes indicates that the modulus of SA 0.2M $CaCl_2$ is compromised at a longer immersion time. This is because prolonged immersion times may lead to increased water absorption, affecting the mechanical properties of the film. Water absorption can act as a plasticizer, reducing the overall strength and stiffness of the material. It was discovered that immersing the SA film in 0.8M $CaCl_2$ significantly increased the elastic modulus of the crosslinked SA from 486.6MPa to 550.5MPa, which is equivalent to a 13% increase over uncrosslinked SA. Even with an increase in immersion time from 4 min to 12 min, the elastic modulus of 0.8M crosslinked SA remained almost constant.

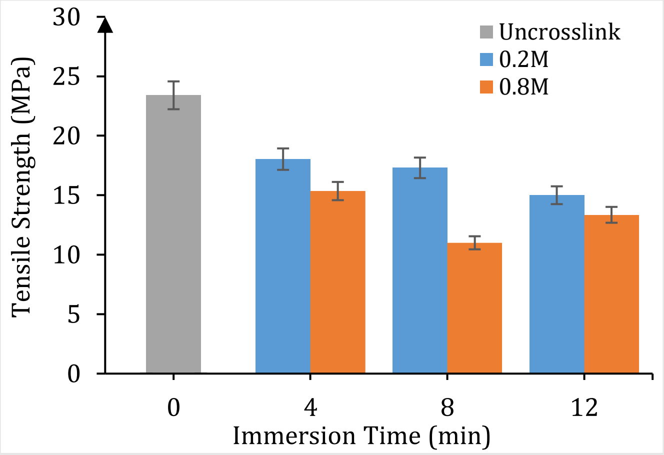

Figure 4. The tensile strength of SA with different $CaCl_2$ concentrations and immersion time.

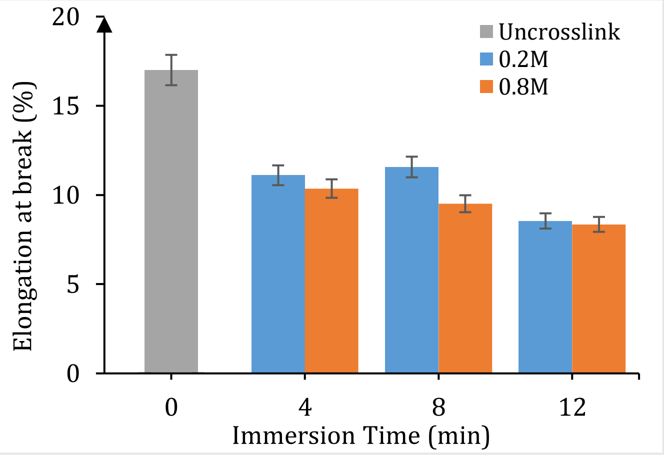

Figure 5. The elongation at break of SA with different $CaCl_2$ concentrations and immersion time.

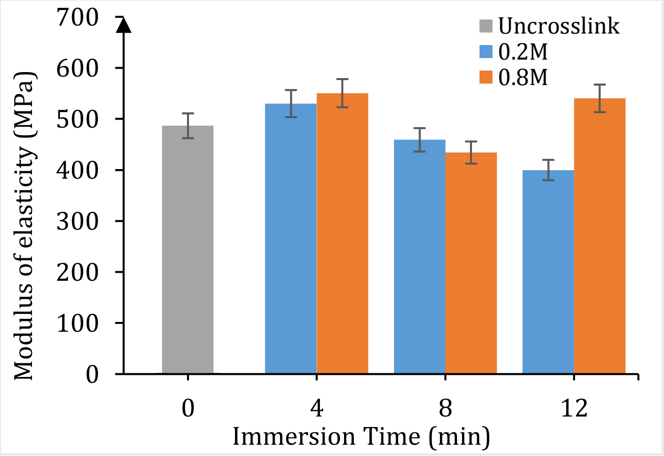

Figure 6. The modulus of elasticity of SA with different $CaCl_2$ concentrations and immersion time.

3.4. Crystallization Behaviour of Uncrosslinked SA, Crosslinked SA and SA/GNP Nanocomposites Film

Based on Figure 7, there are 4 prominent peaks found where the highest peak is found at 22.66° and the second highest peak at 34.29°. Another two small peaks is observed at 47.94° and 53.74°. The amorphous region has been detected for the uncrosslinked SA film at 12.95°, but this amorphous region diminished after being crosslinked using $CaCl_2$. Table 3 shows the crystallinity of uncrosslinked SA, crosslinked SA and SA/GNP nanocomposites film. Uncrosslinked SA film is known to have the lowest degree of crystallinity (24.63%) represented by the existence of a broad and poorly defined diffraction pattern. SA 0.2M-12min, SA 0.8M-4min and SA 0.8M-12min have similarities in the diffraction patterns with the crystallinity 35.11%, 25.78% and 30.02% respectively.

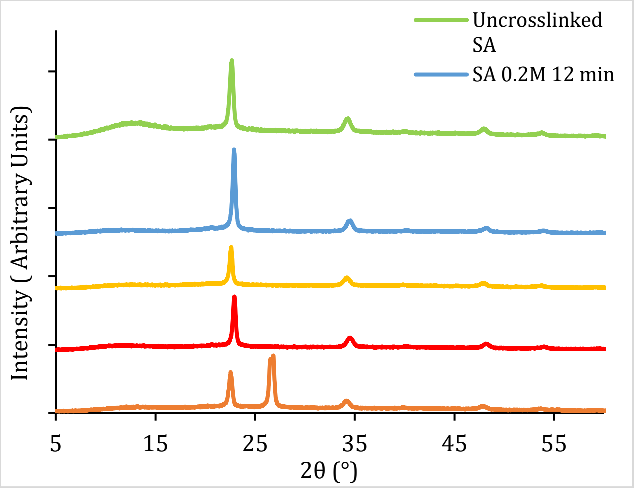

Figure 7. XRD pattern of uncrosslinked SA, crosslinked SA and SA/GNP nanocomposites film.

At a constant immersion time (12 min), the SA films with 0.2M $CaCl_2$ concentrations have higher crystallinity than those with higher concentrations (0.8M). Higher concentrations of crosslinker can lead to faster crosslinking reactions, and in some cases, the reaction may be so rapid that it does not allow for complete crosslinking. Incomplete crosslinking can result in the formation of a more amorphous structure rather than a well-organized, crystalline one.

While at fixed 0.8M of $CaCl_2$, the SA film with a 12-minute immersion time (35.11%) has higher crystallinity than the SA film with a 4-minute immersion time (25.78%). This is because longer immersion times provide more time for the crosslinking reaction to occur. The cross-linking process involves the formation of bonds between polymer chains, leading to the creation of a three-dimensional network structure. As the crosslinking reaction progresses, it may contribute to a more ordered and crystalline arrangement of polymer chains.

Table 3 shows the addition of GNP increases the crystallinity of SA film. SA/GNP film has the highest crystallinity at 40.21% compared to uncrosslinked SA and crosslinked SA. This is because GNP act as a nucleating agent for the SA matrix and accelerated crystallization and increases the crystallinity [10]. In contrast to the other samples, the XRD analysis of SA/GNP nanocomposites reveals a distinct pattern with a sharp and highly intense peak at 26.82°.

Table 3 The crystallinity of uncrosslinked SA, crosslinked SA and SA/GNP nanocomposites film

Sample	Crystallinity (%)
Uncrosslinked SA	24.63
SA 0.2M-12min	35.11
SA 0.8M-4min	25.78
SA 0.8M-12min	30.02
SA/GNP12	40.21

3.5. Chemical Structural Analysis of Uncrosslinked SA, Crosslinked SA and SA/GNP Nanocomposites Film

Figure 8 shows the FTIR spectra of uncrosslinked SA, SA with different of concentrations $CaCl_2$, immersion time and SA/GNP nanocomposites film. Stretching vibrations of the -OH, -C-O-C-, and -CH bonds, respectively, were attributed to the peaks at 3207 cm^{-1}, 1017 cm^{-1}, and 2926 cm^{-1}, respectively. The asymmetrical and symmetric stretching vibrations of the carboxylate group were identified as the sources of the high peak at 1591 cm^{-1} and a little lesser peak at 1406 cm^{-1}, respectively. The two peaks at 1591 cm^{-1} and 1406 cm^{-1}, in particular, were the most relevant characteristic peaks for analysing the ion crosslinking process. It is clear that the asymmetric -COO- peak shifted to a higher wavenumber (from 1591 cm^{-1} to 1592 cm^{-1}/1593 cm^{-1}/1580 cm^{-1}) and the symmetric -COO- peak shifted to a higher wavenumber (from 1406 cm^{-1} to 1413 cm^{-1}/1414 cm^{-1}) when the SA film was crosslinked with Ca^{2+}. This is because of the strong electrostatic interaction between Ca^{2+} and the carboxylic group of alginates [9]. Figure 9 illustrates the proposed SA–GNP interactions in the SA nanocomposites systems crosslinked by using $CaCl_2$.

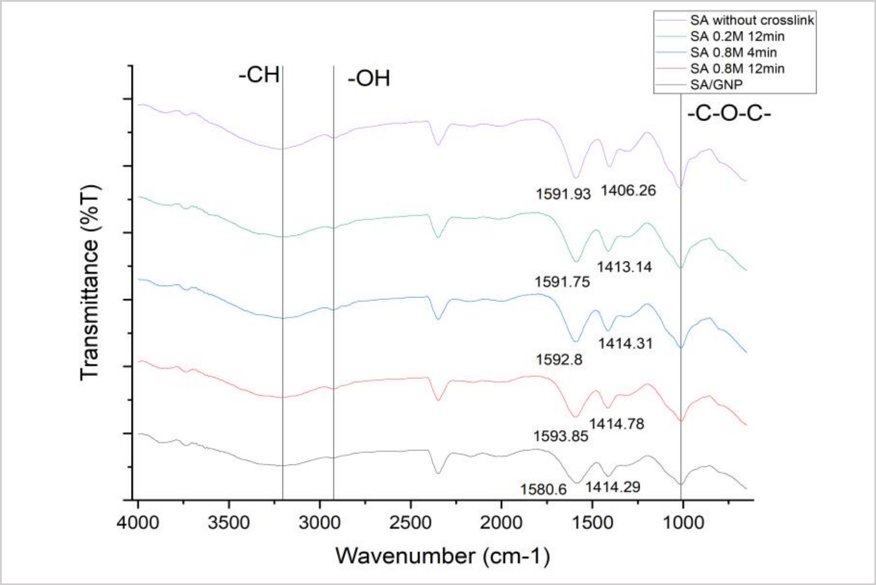

Figure 8. FTIR spectra of uncrosslinked SA, crosslinked SA and SA/GNP nanocomposites film.

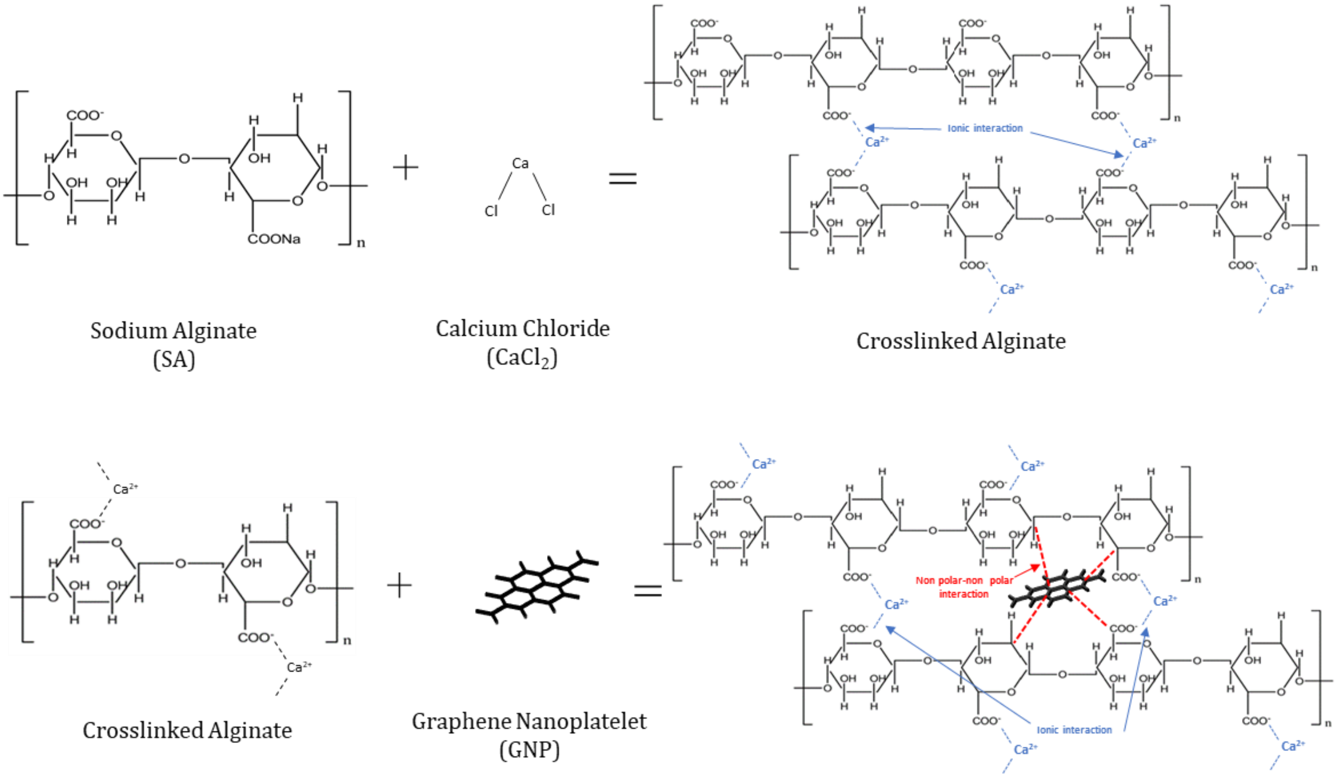

Figure 9. Proposed interactions between the SA chains with $CaCl_2$ and GNP in the SA/GNP nanocomposites system.

3.6. Mechanical Properties of SA/GNP Nanocomposites Film

Based on the ideal parameter (lowest swelling degree and highest gel content) found in the previous section, 0.8M concentration of $CaCl_2$ and 12 minutes immersion time were selected to prepare pristine SA and SA/GNP nanocomposites in this section. Figure 10 demonstrates the tensile strength of SA/GNP nanocomposites with different GNP loading. The tensile strength of pristine SA was 11.93 MPa. By adding as low as 4 wt.% of GNP, the values increased to 14.83 MPa, which is equivalent to a 24% increase compared to pristine SA. GNP have a high aspect ratio and excellent mechanical properties. When incorporated into SA films, GNP can act as reinforcement agents, improving the structural integrity of the nanocomposites. The strong and stiff nature of graphene enhances the overall strength of the film, contributing to higher tensile strength. Furthermore, the surface properties of GNP can facilitate strong interactions with the polymer matrix (SA). Good interfacial adhesion between the GNP and the SA enhances the load transfer between the two phases, leading to better stress distribution and improved tensile strength. The two-dimensional nature of

GNP also allows them to form a barrier within the polymer matrix. This barrier effect can hinder the movement of polymer chains and prevent crack propagation, thereby enhancing the film's resistance to deformation and increasing tensile strength. However, as the loading of GNP further increases from 4 wt.% to 16 wt.%, the tensile strength of the SA/GNP nanocomposites showed a decreasing trend. This might be due to the GNP being poorly dispersed and acting as stress concentrator that can reduce the tensile strength.

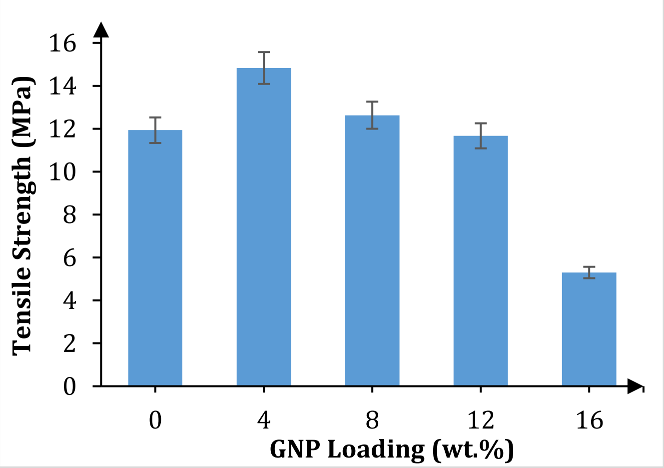

Figure 10. The tensile strength of SA/GNP nanocomposites film with different GNP loading.

Figure 11 demonstrated that the addition of GNP reduced the elongation at the break of the SA/GNP nanocomposites. The elongation at break of SA/GNP nanocomposites was significantly reduced from 8.4% to 5.4% by increasing GNP loading from 0 wt.% to 16 wt.%. This is equivalent to a 36% decrease when compared to pristine SA film. This is due to the GNP's large surface area and strong interactions, which restrict the movement of polymer chains in SA. This limitation in chain mobility can hinder the ability of the material to undergo extensive stretching before reaching the point of failure, leading to a reduction in elongation at break [11, 12].

As shown in Figure 12, the modulus of elasticity for SA/GNP nanocomposites follows a similar trend as compared to the tensile strength result. The modulus of SA/GNP nanocomposites significantly increased to 644.03 MPa after being loaded with 4 wt.% of GNP, which is equivalent to a 57% increase compared to the pristine SA. This indicates that the addition of GNP nanofiller will increase the stiffness and modulus of SA films [13]. However, the elastic modulus of the SA/GNP nanocomposites was reduced from 644.03 MPa to 363.1 MPa after 12 wt.% GNP was added to the matrix. This decreasing trend suggests that the modulus of SA nanocomposites will be compromised when subjected to elevated GNP concentrations. GNP is prone to aggregates due to its high surface energy, resulting in stress concentration and a reduced modulus of elasticity.

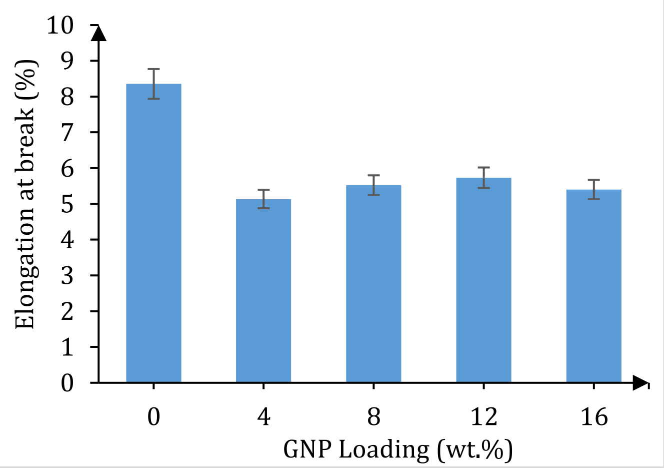

Figure 11. The elongation at break of SA/GNP nanocomposites film with different GNP loading.

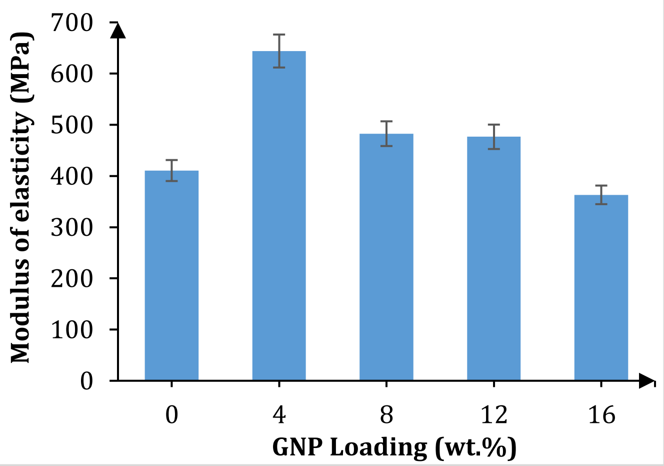

Figure 12. The modulus of elasticity of SA/GNP nanocomposites film with different GNP loading.

3.7. Electrical Conductivity of SA/GNP Nanocomposites Film

The electrical conductivity of the SA/GNP nanocomposites films was measured using a two-probe method to determine the effect of GNP loading on the nanocomposites' electrical conductivity properties. Table 4 shows the electrical conductivity of SA/GNP nanocomposites film with different GNP loading. Figure 13 shows the electrical conductivity of the SA/GNP nanocomposites with different GNP loading using the magnetic stirring method. At the beginning, pristine SA has an electrical conductivity of -7.41 S/cm. According to Figure 13, SA/GNP nanocomposites exhibit increasing electrical conductivity as GNP loading increases. The results show that the electrical conductivity of SA/GNP nanocomposites slightly increases with the addition of 4 wt.% GNP. Further addition of GNP up to 8 wt.%, significantly increases the electrical conductivity to -5.40 S/cm. The SA nanocomposites containing 12 wt.% of GNP achieved the highest electrical conductivity (-5.31 S/cm) because there is perfectly adequate GNP present to form a conductive path. A conductive path within the SA/GNP structure serves as an electron's highway, enabling it to move more easily and face less resistance. As a result, electrical conductivity increases.

Table 4. Electrical conductivity of SA/GNP nanocomposites film

Sample	GNP loading (wt.%)	Log electrical conductivity (S/cm)
Pristine SA	0	-7.41
SA/GNP4	4	-6.98
SA/GNP8	8	-5.40
SA/GNP12	12	-5.31

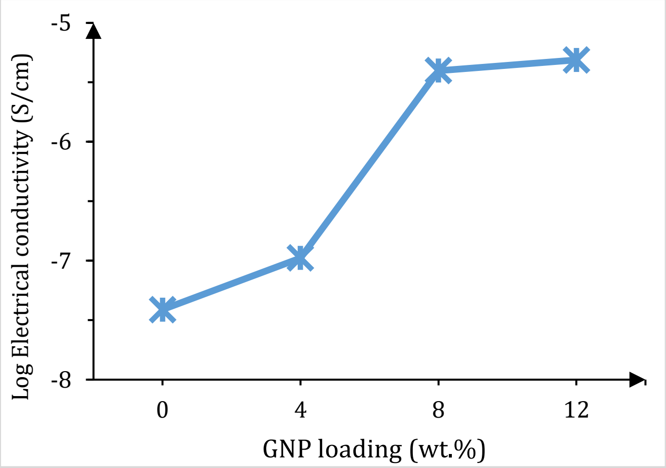

Figure 13. The electrical conductivity of SA/GNP nanocomposites film with different GNP loading.

4. CONCLUSIONS

The research was conducted to observe the effect of $CaCl_2$ concentration and GNP loading on the electrical conductivity, mechanical, physical, crystalline, and chemical structure. Based on the swelling test, the swelling percentage decreases when the immersion time in 0.2M concentration of $CaCl_2$ increases. Besides that, only 12 min immersion time in 0.8M concentration of $CaCl_2$ has the lowest swelling degree with 93.69%. 0.8M concentration of $CaCl_2$ and 12 min immersion time was selected to crosslink the SA/GNP nanocomposites. For the gel fraction, the gel content increases when the concentration of $CaCl_2$ and immersion time increases. Moreover, the GNP loading improved the electrical conductivity of SA/GNP nanocomposites. Mechanical properties of the SA with different concentrations of $CaCl_2$ show that the SA in 0.8M concentration of $CaCl_2$ has a higher elastic modulus than 0.2M concentration of $CaCl_2$ because of higher crosslink density. Mechanical properties of SA/GNP nanocomposites were increased when the GNP loading increased. The inclusion of crosslinker and GNP enhanced the crystallinity of SA films. FTIR does not show much difference in peak for the SA when the concentration of $CaCl_2$, immersion time and GNP loading increase.

ACKNOWLEDGMENTS

The authors would like to acknowledge the financial support from the Fundamental Research Grant Scheme (FRGS) under grant number FRGS/1/2020/TK0/UNIMAP /03/11 from the Ministry of Higher Education Malaysia. The lab facilities were provided by the Faculty of Chemical Engineering Technology, Universiti Malaysia Perlis. Special thanks to those who contributed to this project directly or indirectly.

REFERENCES

[1] E. A. MacGregor, "Biopolymers," in *Encyclopedia of Physical Science and Technology*, R. A. Meyers, Ed., Third Edition ed, 2003, pp. 207-245.

[2] L. P. Amenorfe, E. S. Agorku, F. Sarpong, and R. B. Voegborlo, "Innovative exploration of additive incorporated biopolymer-based composites," *Scientific African,* p. e01359, 2022.

[3] A. J. Teo, A. Mishra, I. Park, Y.-J. Kim, W.-T. Park, and Y.-J. Yoon, "Polymeric biomaterials for medical implants and devices," *ACS Biomaterials Science & Engineering,* vol. 2, no. 4, pp. 454-472, 2016.

[4] A. Zotti, S. Zuppolini, A. Borriello, and M. Zarrelli, "Polymer nanocomposites based on Graphite Nanoplatelets and amphiphilic graphene platelets," *Composites Part B: Engineering,* p. 110223, 2022.

[5] G. Hoti *et al.*, "Effect of the cross-linking density on the swelling and rheological behavior of ester-bridged β-cyclodextrin nanosponges," *Materials,* vol. 14, no. 3, p. 478, 2021.

[6] M. J. Costa, A. M. Marques, L. M. Pastrana, J. A. Teixeira, S. M. Sillankorva, and M. A. Cerqueira, "Physicochemical properties of alginate-based films: Effect of ionic crosslinking and mannuronic and guluronic acid ratio," *Food hydrocolloids,* vol. 81, pp. 442-448, 2018.

[7] H. F. G. Jr, J. R. W. Jr, and E. M. M. III, "Polymer Overview and Definitions," in *Extrusion: The Definitive Processing Guide and Handbook*(Plastics Design Library: William Andrew, Inc., 2005, pp. 165-177.

[8] S. F. Ibrahim, N. A. N. Mohd Azam, and K. A. Mat Amin, "Sodium alginate film: The effect of crosslinker on physical and mechanical properties," in *IOP Conference Series: Materials Science and Engineering*, 2019, vol. 509, p. 012063: IOP Publishing.

[9] J. Li, Y. Wu, J. He, and Y. Huang, "A new insight to the effect of calcium concentration on gelation process and physical properties of alginate films," *Journal of Materials Science,* vol. 51, pp. 5791-5801, 2016.

[10] Y. Ming, Z. Zhou, D. Xu, R. Liu, Y. Nie, and T. Hao, "The effect of molecular weight of polymers grafted in two-dimensional filler on crystallization behaviors studied by dynamic Monte Carlo simulations," *Computational Materials Science,* vol. 155, pp. 144-150, 2018.

[11] L. Kean Chong, A. F. Osman, A. A. Ahmad Fauzi, A. A. Alrashdi, and K. A. Abdul Halim, "The Mechanical and Thermal Properties of Poly (ethylene-co-vinyl acetate)(PECoVA) Composites with Pristine Dolomite and Organophilic Microcrystalline Dolomite (OMCD)," *Polymers,* vol. 13, no. 18, p. 3034, 2021.

[12] K. Lim, N. Halim, S. Mahamud, A. Osman, M. Pisal, and A. Masa, "Mechanical properties of poly-(hydroxybutyrate-co-valerate)/natural rubber/cellulose nanocrystal (PHBV/NR/CNC) nanocomposites prepared by using two-roll mill method," in *AIP Conference Proceedings*, 2024, vol. 2883, no. 1: AIP Publishing.

[13] E. Tarani *et al.*, "Influence of graphene platelet aspect ratio on the mechanical properties of HDPE nanocomposites: Microscopic observation and micromechanical modeling," *Polymers,* vol. 12, no. 8, p. 1719, 2020.